

Photocatalytic Nanowires-Based Air Filter: Towards Reusable Protective Masks

Endre Horváth, Lídia Rossi, Cyprien Mercier, Caroline Lehmann, Andrzej Sienkiewicz, and László Forró*

In the last couple decades, several viral outbreaks resulting in epidemics and pandemics with thousands of human casualties have been witnessed. The current Covid-19 outbreak represents an unprecedented crisis. In stopping the virus' spread, it is fundamental to have personal protective equipment and disinfected surfaces. Here, the development of a TiO₂ nanowires (TiO₂NWs) based filter is reported, which it is believed will work extremely well for personal protective equipment (PPE), as well as for a new generation of air conditioners and air purifiers. Its efficiency relies on the photocatalytic generation of high levels of reactive oxygen species (ROS) upon UV illumination, and on a particularly high dielectric constant of TiO₂, which is of paramount importance for enhanced wettability by the water droplets carrying the germs. The filter pore sizes can be tuned by processing TiO₂NWs into filter paper. The kilogram-scale production capability of TiO₂NWs gives credibility to its massive application potentials.

1. Introduction


The threats coming from microorganisms, viruses and bacteria are getting more frequent and more devastating lately, primarily due to the highly increased mobility of people and goods, which enhances the spread of infections. One may have in mind the outbreak of SARS-CoV in 2004^[1–6] of H1N1 in 2009,^[7–9] and the Ebola virus in 2018.^[10–12] In the case of bacteria, the O104:H4 strain of *Escherichia coli*^[13–16] caused casualties, but the danger is also coming from antibiotics resistant species like *Legionella* bacteria,^[17–19] *Klebsiella pneumoniae*,^[20–23] and *Staphylococcus aureus*.^[24–27]

The most sinister actuality is the pandemic outbreak of Covid-19, caused by the highly contagious coronavirus SARS-CoV-2. It has rapidly spread worldwide, leading to infections on

Dr. E. Horváth, Dr. L. Rossi, C. Mercier, Dr. A. Sienkiewicz, Prof. L. Forró
Laboratory of Physics of Complex Matter
Ecole Polytechnique Fédérale de Lausanne
Lausanne 1015, Switzerland
E-mail: laszlo.forro@epfl.ch

C. Lehmann
Laboratory of Physics of Living Matter
Ecole Polytechnique Fédérale de Lausanne
Lausanne 1015, Switzerland

Dr. A. Sienkiewicz
ADSresonances
Préverenges 1028, Switzerland

 The ORCID identification number(s) for the author(s) of this article can be found under <https://doi.org/10.1002/adfm.202004615>.

DOI: 10.1002/adfm.202004615

a millions-scale, along with hundreds of thousands of human losses.^[28]

As if today, the world is far behind in finding an efficient fight against this disease. Our society needs to employ all possible means in reducing the number of infections and mortalities.

In this struggle, one possibility is to create specialized surfaces, which by photophysical effects could damage and disable airborne pathogens such as bacteria and viruses,^[29] as well as SARS-CoV-2. The bactericidal-virucidal surfaces suggested herein have potential applications in air filtering systems such as air conditioners, and most importantly in the fabrication of personal protective masks. Filters made of photocatalytic materials that generate high levels of reactive oxygen

species (ROS) upon UV light illumination, could not only efficiently inactivate airborne pathogens, but would also offer the benefits of reusability.

From this perspective, TiO₂-based photocatalytic materials represent a very promising solution for the above-mentioned field of applications.^[30–36] Most explicitly, enhanced photocatalytic properties are expected from nanoparticulate forms of TiO₂, such as TiO₂ nanoparticles (TiO₂NPs) and 1D TiO₂ nanostructures, like nanowires (TiO₂NWs) or nanotubes (TiO₂NTs), which offer a much larger specific surface area than bulk and polycrystalline counterparts.^[37,38] It has been demonstrated that the high surface-to-volume ratio of 1D TiO₂ nanostructures leads to a marked decrease in the hole–electron recombination rate, as well as to a faster interfacial charge carrier transfer rate. Both of these factors are favorable for enhancing the photocatalytic activity of 1D nanoparticulate forms of TiO₂.^[39]

It is also worth mentioning that, due to free electrons' high mobility in the air, both virus-laden water microdroplets and single airborne microorganisms often accumulate a noticeable negative charge. Therefore, the high dielectric constant of TiO₂—with its concomitant large charge-storage capacity—contributes to the enhanced electrostatic precipitation of the droplets on the nonwoven network of TiO₂NWs. Moreover, the presence of numerous Ti³⁺ sites on the surface or TiO₂NWs, previously reported by us,^[40] is highly favorable for water adsorption, leading to super-hydrophilicity at the macroscale.^[41] Therefore, the super-hydrophilicity of TiO₂NWs-based filtering materials causes water droplets to adhere and spread on the TiO₂ surface, aiding in filtration.

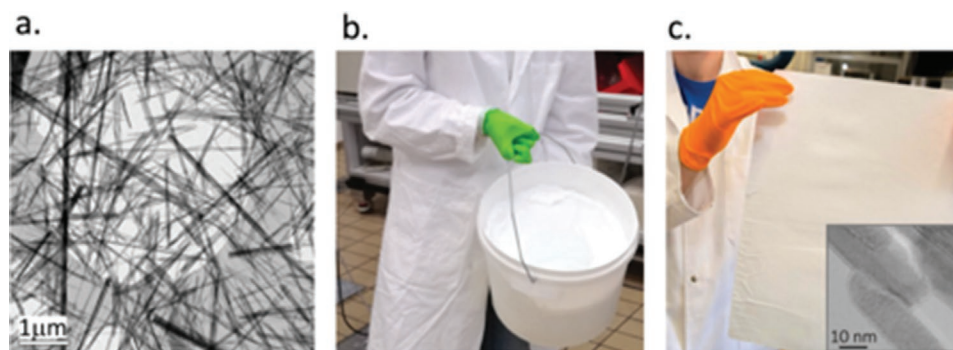


Figure 1. a) SEM image of an assembly of titanate NWs ($\text{H}_2\text{Ti}_3\text{O}_7$), the precursor of TiO_2 anatase NWs. b) The upscale of the synthesis occasioned titanate NWs production on kg per day level; c) the processing (spreading and thermal treatment) results in a filter paper of TiO_2 NWs. The inset shows TEM image of the fused NWs as the result of calcination procedure.

Thus, all things considered, the TiO_2 NWs are very suitable for preparing larger photocatalytic surfaces because they also have an ideal shape for assembly into nanoporous aerogel membranes.^[42] We here report on the feasibility of producing a reusable photocatalytically active filter paper from TiO_2 NWs. We also provide a thorough characterization of this composite material in terms of its high propensity toward photogeneration of ROS, and the degradation of microbiological pathogens.

2. Results and Discussion

2.1. Synthesis

The herein presented elaboration of a practical and reliable large-scale synthesis of TiO_2 NWs represents a breakthrough strategy toward the fabrication of photocatalytic materials suitable for preparing easily sterilizable air filters, including reusable protective masks.

Titanium oxide nanowires are normally attained via hydrothermal synthesis, where nanoparticles of TiO_2 are treated in a closed vessel at high pressures of 140–200 °C during several days of reaction time (see **Figure 1a**).^[43–46] Unfortunately, the yield of such synthesis is very low, several few grammes per run, which is a strong handicap for large scale applications.

Through an original synthesis method,^[42] production has been greatly upscaled. In a base solution, Ti containing starting material is added, and the mixture is heated in a base resistive vessel to 70 °C. A shear mixing results the formation of a high fraction of mesoporous titanates, and a lower fraction of macroporous material. The textural properties can be tuned by temperature, with and by the time of shear mixing. After the synthesis, the jelly titanium oxide composite (see **Figure 1b**) is transferred into a press or centrifuge to separate it from the residues of the reaction. In a single shot the quantity of titanate NWs is in the 0.3–1 kg range.

The NWs can be processed into films by doctor blading, screen printing, filtering, dip coating, and spin coating with a thickness less than 2 μm .^[47] The film can be removed from the support if the support is a hydrophobic material. After air drying at 120 °C, calcination and phase transformation from titanate to anatase to rutile occur within a range of 400–1000 °C range.^[48] It results in a freestanding, flexible film, which—depending on

the thickness—could be even transparent.^[49] Note that the calcination fuses the TiO_2 NWs together (see the inset to **Figure 1c** and the Supporting Information), thus resulting in a filter paper, which does not release nanostructures under normal flow conditions.^[37]

This film of TiO_2 NWs filter paper is the starting structure for all water and air filters which, by UV illumination, could be disinfected from viruses, bacteria, and generally all organic species. Here below, the efficiency of TiO_2 NWs and the filter is demonstrated by the photocatalytic ROS generation, as well as the corresponding high potential for DNA degradation and annihilation of *E. coli*, the gold-standard bacteria.

2.2. The Principle

The principle of the filter papers operation is illustrated in **Figure 2**. The pore-sizes of the filter can be tuned during its fabrication process by modifying both the thickness and density of the filter paper (See **Figure S2** of Supporting Information). This can allow for the efficient trapping of pathogens of different sizes, including the smallest viruses (**Figure 2a**).

An important characteristic of the TiO_2 is its high dielectric constant (ϵ) in the 70–80 range, which defines the polaronic nature of the electronic charges in the material.^[50] A high ϵ value is important for the filtering material, since it facilitates wetting the filter's surface by droplets of water or saliva, which could carry the germs.

It is worth mentioning that the presence of moisture, even in the form of humidity traces, is essential for the photocatalytic and antimicrobial activities of the filter paper. It is therefore widely accepted that in an aqueous milieu and upon UV illumination, the TiO_2 -based photocatalytic materials efficiently generate the so-called ROS—that is, hydroxyl radicals ($\text{OH}\cdot$), hydroperoxyl radicals ($\text{HO}_2\cdot$), hydrogen peroxide (H_2O_2), singlet oxygen ($^1\text{O}_2$), and superoxide radicals ($\text{O}_2\cdot^-$).^[51] In particular, the UV-light excited TiO_2 nanoparticles convert the incident photons into electron/hole pairs. These can either recombine, or migrate to the particle's surface, where they can generate ROS and/or activate redox processes.^[52] The plausible mechanisms of photogeneration of various forms of ROS during the UV-light induced stepwise oxidation of water (H_2O), and stepwise reduction of oxygen (O_2) taking place on

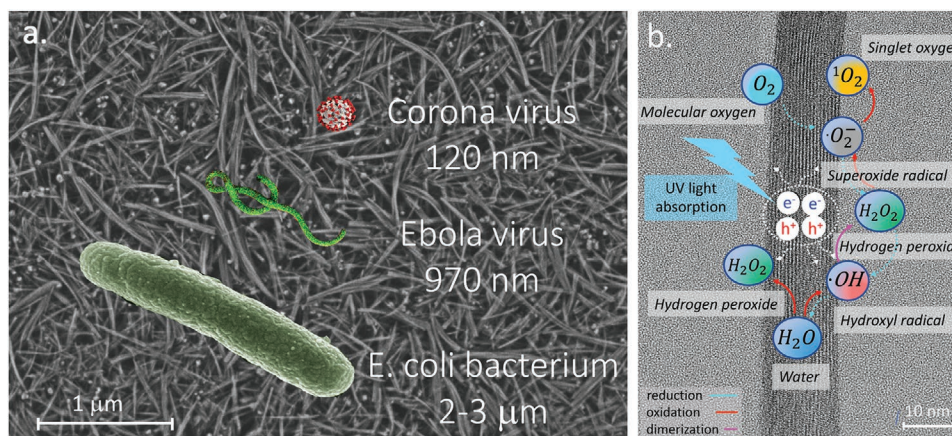


Figure 2. a) The SEM image of the surface of the TiO₂NWs filter overlapped with the schematic representations of the example germs to be filtered out. b) Schematic illustration of photocatalytic processes leading to ROS generation at the humid surface of TiO₂NWs. The resulting photogenerated ROS inactivate all the microbial targets in its proximity.

the surface of the TiO₂NWs, are schematically illustrated in Figure 2b.

In general, OH· radicals are considered the most powerful oxidizing species.^[53,54] They are also believed to be the first responsible for the photodegradation processes of organic micropollutants in aqueous solutions. Although concomitantly photogenerated superoxide radicals (O₂^{·-}) have less oxidizing properties, they still can lead to the formation of other active ROS, including singlet oxygen (¹O₂), which is also very potent.^[51]

The efficiency of the TiO₂NWs and the composed filter paper in producing ROS is demonstrated using several experimental techniques, including electron spin resonance (ESR), degeneration of a biological molecule (DNA) detected by atomic force microscopy (AFM) and gel electrophoresis, as well as by the photocatalytic annihilation of *E. coli* cells tracked by survival counting using UV illumination.

2.3. ESR Study of the ROS Generation on TiO₂NWs Surface upon UV Illumination

The documentation of ROS is a defiant task because of their short lifetime, of the order of 10⁻¹⁰ to 10⁻⁶ s. One of the best methods is to convert them into stable radicals, which could be easily, selectively, and sensitively identified ESR spectroscopy.^[55] This method is based on spin-trapping molecules which react with ROS and change their spin state: either the existing spins are scavenged or they produce stable spin-adducts. Their spectra can be easily integrated and their concentration measured.

The propensity of the herein synthesized TiO₂NWs-based composite to photogenerated ROS was checked in the aqueous milieu using a custom-designed photoreactor (details in the Supporting Information). The sketch of the corresponding experimental setup is overviewed in Figure 3a, with more details given in Supporting Information. Specifically, the inner

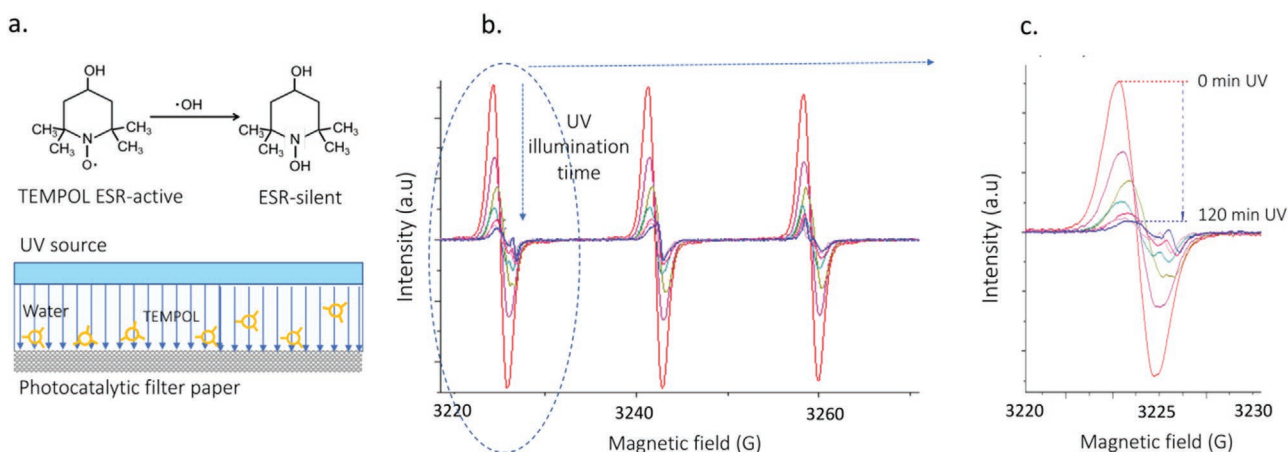


Figure 3. a) Illustration of how ESR can detect and differentiate ROS by using targeted spin traps. Here the TEMPOL molecule loses its spin upon reaction with OH· radicals produced upon UV illumination. The experiment is performed in a photocatalytic cell, where aqueous solution of TEMPOL is circulated, and, when TEMPOL molecules come in close proximity to the TiO₂NWs photocatalytic lining, they are oxidized and become ESR-silent. b) ESR spectra of TEMPOL progressively diminish with increasing illumination time (acquired over 120 min time). c) Zoom on the low-field part of the hyperfine spectrum, which shows the 15-fold decrease of the TEMPOL signal with illumination time, as well as the appearance of TEMPONE at 3225 G.

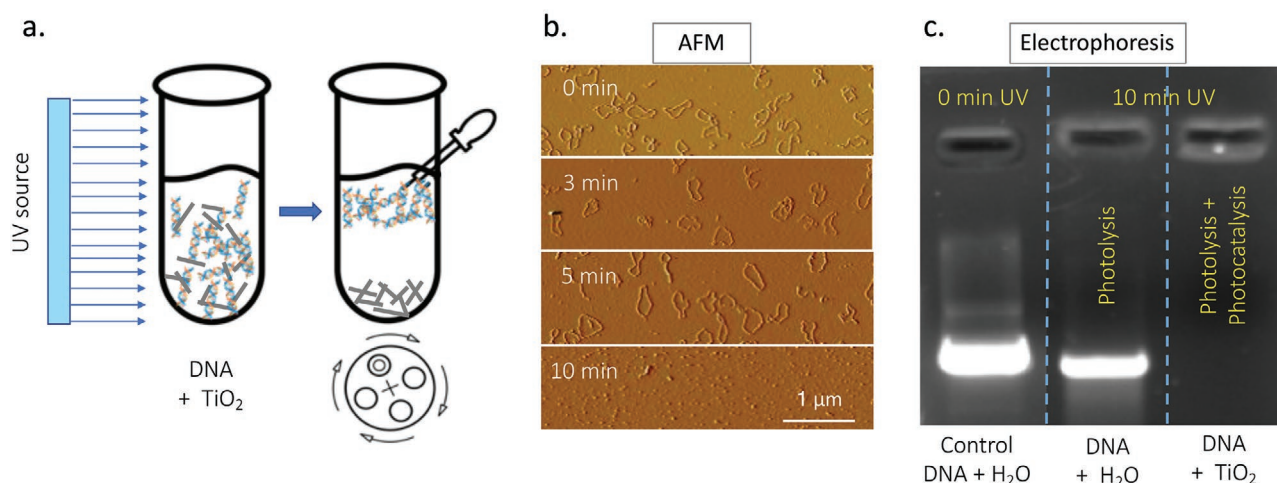


Figure 4. The capability of ROS generated at the surface of TiO₂NWs upon UV illumination to degrade biomolecules is illustrated in the case of strands of DNA. a) The suspension of TiO₂NWs and DNA was illuminated, then centrifuged. Samples for AFM and gel electrophoresis were pipetted from the top of the suspension. b) The AFM images of the DNA molecules deposited on a mica surface show their progressive fractionalization with increasing illumination times. c) The photocatalytic degradation of the DNA is confirmed by electrophoresis; also shown are the two control experiments for DNA suspensions in the absence of contact with TiO₂NWs, performed in the dark and under UV light (only photolysis).

wall of the tubular photoreactor was covered with the TiO₂NWs-based composite material, thus forming a photocatalytic lining. The built-in commercially-available UV lamp (Hamatsu, $\lambda = 365 \text{ nm}$ of 16 mW cm^{-2}) served as a UV light source for inducing the photocatalytic processes at the surface of the TiO₂NWs-based photocatalytic lining.

The stable nitroxide radical, 4-hydroxy-2,2,6,6-tetramethylpiperidine-1-oxyl (called TEMPOL), was used as a target molecule for the photogenerated OH· and O₂·− radicals. It is well known that the ESR-active TEMPOL is a water-soluble antioxidant, reportedly acting as a superoxide dismutase (SOD) mimicking agent.^[56] In particular, reactive pathways of TEMPOL with O₂·− and OH· radicals have been reported to introduce structural changes at the 1- and 4-positions of the TEMPOL molecule, respectively.^[57,58] Acting in concert, these structural changes induce both the decay of the ESR-active TEMPOL, as well as the concurrent formation of another ESR-active radical, 4-oxo-TEMPO, i.e., TEMPONE. In Figure 3 photocatalytic decomposition of TEMPOL is shown (the TEMPONE case is given in the Supporting Information).

In aqueous solutions, TEMPOL reveal easily detectable ESR spectra, which are characteristic for NO-centered radicals bearing one unpaired electron ($S = 1/2$). In particular, the corresponding ESR signals consist of three well resolved features resulting from the ¹⁴N atom-related hyperfine splitting ($I = 1$). Due to small differences in hyperfine splitting constants— $A^{14}\text{N}$, and spectroscopic g -factor values, of $17.1 \text{ G/g} = 2.0057$ for TEMPOL and $16.1 \text{ G/g} = 2.0056$ for TEMPONE—these two nitroxide radicals can be very easily distinguished.

The time-course of 0–120 min for the photocatalytic decomposition of TEMPOL in the presence of the synthesized TiO₂NWs-based photocatalytic material is shown in Figure 3b. As can be seen, the characteristic ESR signal of TEMPOL rapidly decays as a function of time of exposure to the UV light in the photoreactor. Over 120 min of the exposure time, the overall ESR signal intensity of TEMPOL decays by a factor

of ≈ 15 . With the photoinactivation of TEMPOL, a concurrent process of the formation of TEMPONE can also be observed (Figure 3c, the weak signal at 3255 G). These two processes—the decay of TEMPOL and the progressive increase of TEMPONE—prove that under UV light exposure the herein synthesized TiO₂NWs-based photocatalytic material generates O₂·− and OH· radicals.

2.4. AFM and Electrophoresis Demonstration of the DNA Rupturing by ROS

After demonstrating that TiO₂NWs can very efficiently generate ROS, we checked its effect on an important biomolecule, the DNA, in an experimental configuration described in the Supporting Information. We used a commercial DNA pUC19, which after treatment with an enzyme remain stayed open, and not supercoiled, with a length of 913 nm. A suitable solution of TiO₂NWs and DNA was exposed to 365 nm UV radiation (see sketch in Figure 4a), with a particular cycle (30 s of irradiation followed by 2 min of shaking and rotation without irradiation) to avoid overheating which could lead to false results.

Variable exposure times to UV illumination were employed: 3, 5, 10, and 15 min. The TiO₂/DNA solution was finally deposited, with a suitable procedure, see Supporting Information paragraph 4, on a smooth mica substrate for AFM observation.

The AFM imaging technique made it possible to observe the presence or disappearance of the DNA strands in a very local area. In particular, the tapping mode AFM images shown in Figure 4b clearly demonstrate that, with increasing illumination times, the DNA strands are being progressively degraded and, after 10 min of exposure, only their debris could be detected.

This observation is concomitant with the gel electrophoresis experiment. DNA strands and their fragments migrate through the agarose gel with different velocities, v , where $v = E \times z/f$. These velocities result from the differences in the strength of

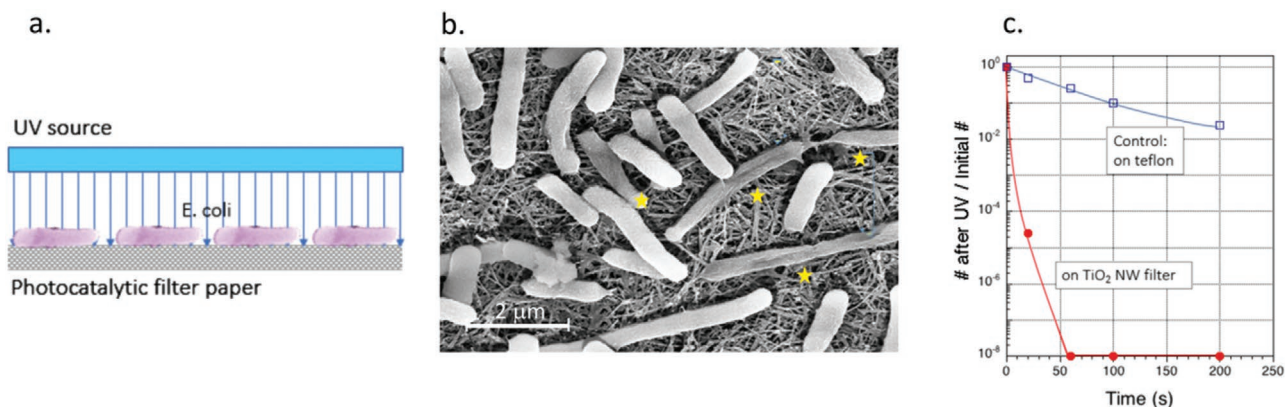


Figure 5. The effect of the TiO₂NWs photocatalytic filter on *E. coli* bacteria. a) Scheme showing *E. coli* bacteria deposited on the humid surface of the TiO₂NWs filter and exposed to UV light. b) SEM image of the TiO₂NWs photocatalytic filter with the deposited *E. coli* bacteria acquired after 30 s of UV-light exposure; the most heavily damaged bacteria are indicated by the yellow stars. c) The comparison of the TiO₂NWs filter's bacterial inactivation performance, and the control surface of the humid Teflon filter, performed by bacterial count at discrete illumination times.

the local electric field (E), the net charge (z), and the friction force (f). The latter parameter, f , is a quantity dependent on the DNA strand size.

The location of the DNA strands and their fragments in the gel was visualized by means of attaching a suitable fluorescent dye, GelRed from Biotium. One can see (Figure 4c) that in the case of no UV exposure, the DNA strands are slowly spreading in the gel due to their large sizes and important friction. In contrast, due to low friction from their small size, after 15 min of UV exposure small DNA debris quickly moved to the upper side of the gel.

As can also be seen in Figure 4c, the control electrophoresis experiments for DNA suspended in distilled water, in the absence of contact with TiO₂NWs and performed both in the dark and under UV light illumination, did not reveal any marked fragmentation of the DNA strands. Thus, the potential photolytic impact of the uniquely employed UV light turned out to be quite negligible as compared to the synergetic photocatalytic action of TiO₂NWs and UV illumination.

In brief, the electrophoresis experiments performed on the DNA strands corroborate the ESR and AFM studies results, which both point to the strength of TiO₂NWs photocatalytic action when exposed to UV light illumination.

2.5. The Efficiency of the TiO₂NWs Photocatalytic Filter in the Case of *E. Coli*

The next step was testing the TiO₂NWs-based filters performance in killing microorganisms. By the filtering action, these can be stopped as they adhere to the fibers of humid TiO₂NWs. Humidity is always present under typical daily conditions, especially if such a filter paper is used for air-conditioning applications, where, after switching the air-conditioner off, the water condensation commonly occurs. Such an environment is therefore favorable for bacterial proliferation, unless it is disinfected by UV light.

Here, we used the reference bacteria for such studies, the *E. coli*. From a bacterial suspension of known concentration of

2×10^8 CFU per mL, a volume of 5 μL was dropped on the filter surface (see the illustration in Figure 5a) and exposed to illumination at 365 nm wavelength from a UV light source with a power density of 16 mW cm^{-2} , for discrete time intervals of 20, 60, 100, and 200 s. After each illumination run, the *E. coli* was washed off the membranes by placing them in Eppendorf tubes containing physiological salt, and rinsing for 60 min to retrieve the survived cells back into solution. Next, serial dilutions were prepared from the solution containing cells/membrane, and 10 μL of each dilution was spotted on LB agar plates. Agar plates were incubated overnight at 37 °C. The cell concentration per mL (CFU per mL) was extrapolated from the colonies counted at the appropriate spots for TiO₂NWs membrane, from which the survival rate could be determined. In the control experiment, non-UV exposed *E. coli* bacteria were washed off the TiO₂NWs filter paper and underwent the same protocol, thus making it possible to reproduce the initial concentration of bacteria.

As can be seen in the scanning electron microscopy (SEM) image in Figure 5b, already after the initial exposure to UV light for 30 s, numerous damaged bacteria could be identified, as highlighted by the yellow stars in this figure. Clearly, the actual population of nonviable (inactivated) cells was markedly larger.

Consequently, for the experiment performed on the surface of the TiO₂NWs filter paper, after 60 s of UV light exposure one can hardly identify any bacteria which could still proliferate (red trace in Figure 5c). Although the control experiment performed with *E. coli* bacteria on the wet Teflon filter surface reveals some photodegradation (blue trace in Figure 5c), the actual degree of bacterial photoinactivation is definitely non-commensurable with the one observed for the TiO₂NWs-based photocatalytic filter. This points to the extreme efficiency of our TiO₂NWs filter paper in killing bacteria. This filter paper may also kill other microbial pathogens, such as viruses, which can be filtered out and photocatalytically inactivated at its surface.

One could also notice that the deleterious effects of UV exposures are occurring at different timescales: for the ESR experiments with TEMPOL it is of 120 min, while for the *E. coli* bacteria it rather happens on a timescale of 120 s. This is due to



Figure 6. The reusable protective mask designed around the TiO_2NWs -based filter paper. a) Photo of the mask prototype in which the TiO_2NWs filter paper is attached to a 3D-printed plastic frame. b) Photo of the mask prototype during its disinfection under 365 nm UV illumination. The filtered germs are inactivated by ROS, formed in the photocatalytic reaction on the surface of the filter material. c) Photo of the reusable protective mask prototype in real conditions (courtesy of Swoxid S.A.).

the fact that ROS, although extremely reactive, are short-lived, and correspondingly, their radius of action is very limited. Thus, the mutual distances between the biological species and TiO_2NWs are important. The *E. coli* bacteria are anchored to the filter surface, so the effect of ROS is very efficient, while for the ESR, the organic molecules pass by in flow condition. For the AFM and electrophoresis studies, the DNA and TiO_2NWs are in a confined space, and the timescale is intermediate to the two other configurations.

3. Conclusion and Outlook

The immediate importance of such a filter is rendered by the Covid-19 crisis urgency, which has rapidly spread into a pandemic. Since the transmission routes of its vector, SARS-CoV-2 virus, are still far from understood, wearing personal protective masks is of great importance.^[59] Moreover, according to some health experts, the currently used disposable facemasks do not block all pathogens, neither can they inactivate the viruses. Thus, used and discarded masks can even become a vector for disease, especially if the virus survives on a disposable mask.

Therefore, easily sterilizable and reusable masks with antiviral properties could provide a potent prevention tool against the rapid spread of SARS-CoV-2 and other coronaviruses that have evolved into more severe illnesses such as SARS and MERS. We estimate that such a TiO_2 NWs based light-sterilizable mask may be reused more than 1000 times. A prototype of such a mask has been developed and is shown in **Figure 6**. Evidently, this design addresses an impending mask shortage crisis. In addition, it should also reduce the

environmental and public health issues related to the millions of masks discarded daily worldwide outside of the medical environment, where infectious and hazardous medical waste is properly treated and disposed.

As of today, the technology we propose, exclusively under laboratory conditions, will allow for the filter production capacity of about 100–200 m^2 per week. This is enough to fabricate 40 000–80 000 reusable masks monthly. Clearly, there is no upper limit of this technology for an industrial production line. It should be mentioned that such a nanoporous photocatalytic filter can also be used for other purposes, such as air conditioners and water purification.^[60]

Supporting Information

Supporting Information is available from the Wiley Online Library or from the author.

Acknowledgements

E.H. gratefully acknowledges the support of the support of Zeno Karl Schindler, MBR Global Water Award, Swiss-African Research Cooperation (SARECO) and Tech4impact Playgrant EPFL. We would also like to thank Lenke Horváth, Rita Smajda, Raphaël Foschia, Giovanni Dietler and Jérôme Gabathuler for their help in the experiments. A special thanks to Claude Marion for his continuous interest for the project.

Conflict of Interest

The authors declare no conflict of interest.

Keywords

E. coli, electron spin resonance, filter, nanowires, photocatalysis, reactive oxygen species, TiO₂

Received: May 29, 2020

Revised: July 2, 2020

Published online: August 7, 2020

- [1] T. G. Ksiazek, D. Erdman, C. S. Goldsmith, S. R. Zaki, T. Peret, S. Emery, S. Tong, C. Urbani, J. A. Comer, W. Lim, P. E. Rollin, S. F. Dowell, A.-E. Ling, C. D. Humphrey, W.-J. Shieh, J. Guarner, C. D. Paddock, P. Rota, B. Fields, J. DeRisi, J.-Y. Yang, N. Cox, J. M. Hughes, J. W. LeDuc, W. J. Bellini, L. J. Anderson, *N. Engl. J. Med.* **2003**, *348*, 1953.
- [2] C. Drosten, S. Günther, W. Preiser, S. van der Werf, H.-R. Brodt, S. Becker, H. Rabenau, M. Panning, L. Kolesnikova, R. A. M. Fouchier, A. Berger, A.-M. Burguière, J. Cinatl, M. Eickmann, N. Escriou, K. Grywna, S. Kramme, J.-C. Manuguerra, S. Müller, V. Rickerts, M. Stürmer, S. Vieth, H.-D. Klenk, A. D. M. E. Osterhaus, H. Schmitz, H. W. Doerr, *N. Engl. J. Med.* **2003**, *348*, 1967.
- [3] K. W. Tsang, P. L. Ho, G. C. Ooi, W. K. Yee, T. Wang, M. Chan-Yeung, W. K. Lam, W. H. Seto, L. Y. Yam, T. M. Cheung, P. C. Wong, B. Lam, M. S. Ip, J. Chan, K. Y. Yuen, K. N. Lai, *N. Engl. J. Med.* **2003**, *348*, 1977.
- [4] N. Lee, D. Hui, A. Wu, P. Chan, P. Cameron, G. M. Joynt, A. Ahuja, M. Y. Yung, C. B. Leung, K. F. To, S. F. Lui, C. C. Szeto, S. Chung, J. J. Y. Sung, *N. Engl. J. Med.* **2003**, *348*, 1986.
- [5] S. M. Poutanen, D. E. Low, B. Henry, S. Finkelstein, D. Rose, K. Green, R. Tellier, R. Draker, D. Adachi, M. Ayers, A. K. Chan, D. M. Skowronski, I. Salit, A. E. Simor, A. S. Slutsky, P. W. Doyle, M. Kraiden, M. Petric, R. C. Brunham, A. J. McGeer, *N. Engl. J. Med.* **2003**, *348*, 1995.
- [6] World Health Organization (WHO), **2003**.
- [7] C. Fraser, C. A. Donnelly, S. Cauchemez, W. P. Hanage, M. D. van Kerkhove, T. D. Hollingsworth, J. Griffin, R. F. Baggaley, H. E. Jenkins, E. J. Lyons, T. Jombart, W. R. Hinsley, N. C. Grassly, F. Balloux, A. C. Ghani, N. M. Ferguson, A. Rambaut, O. G. Pybus, H. Lopez-Gatell, C. M. Alpuche-Aranda, I. B. Chapela, E. P. Zavala, D. M. E. Guevara, F. Checchi, E. Garcia, S. Hugonnet, C. Roth, *Science* **2009**, *324*, 1557.
- [8] R. J. Garten, C. T. Davis, C. A. Russell, B. Shu, S. Lindstrom, A. Balish, W. M. Sessions, X. Xu, E. Skepner, V. Deyde, M. Okomo-Adhiambo, L. Gubareva, J. Barnes, C. B. Smith, S. L. Emery, M. J. Hillman, P. Rivaviller, J. Smagala, M. de Graaf, D. F. Burke, R. A. M. Fouchier, C. Pappas, C. M. Alpuche-Aranda, H. López-Gatell, H. Olivera, I. López, C. A. Myers, D. Faix, P. J. Blair, C. Yu, K. M. Keene, P. D. Dotson, D. Boxrud, A. R. Sambol, S. H. Abid, K. S. George, T. Bannerman, A. L. Moore, D. J. Stringer, P. Blevins, G. J. Demmler-Harrison, M. Ginsberg, P. Kriner, S. Waterman, S. Smole, H. F. Guevara, E. A. Belongia, P. A. Clark, S. T. Beatrice, R. Donis, J. Katz, L. Finelli, C. B. Bridges, M. Shaw, D. B. Jernigan, T. M. Uyeki, D. J. Smith, A. I. Klimov, N. J. Cox, *Science* **2009**, *325*, 197.
- [9] G. J. D. Smith, D. Vijaykrishna, J. Bahl, S. J. Lycett, M. Worobey, O. G. Pybus, S. K. Ma, C. L. Cheung, J. Raghvani, S. Bhatt, J. S. M. Peiris, Y. Guan, A. Rambaut, *Nature* **2009**, *459*, 1122.
- [10] A. Barry, S. Ahuka-Mundede, Y. Ali Ahmed, Y. Allaranger, J. Anoko, B. N. Archer, A. Aruna Abedi, J. Bagaria, M. R. D. Belizaire, S. Bhatia, T. Bokenge, E. Bruni, A. Cori, E. Dabire, A. M. Diallo, B. Diallo, C. A. Donnelly, I. Dorigatti, T. C. Dorji, A. R. Escobar Corado Waeber, I. S. Fall, N. M. Ferguson, R. G. FitzJohn, G. L. Folefack Tengomo, P. B. H. Formenty, A. Forna, A. Fortin, T. Garske, K. A. Gaythorpe, C. Gurry, E. Hamblion, M. Harouna Djingarey, C. Haskew, S. A. L. Hugonnet, N. Imai, B. Impouma, G. Kabongo, O. I. Kalenga, E. Kibangou, T. M.-H. Lee, C. O. Lukoya, O. Ly, S. Makiala-Mandanda, A. Mamba, P. Mbala-Kingebeni, F. F. R. Mboussou, T. Mlanda, V. Mondonge Makuma, O. Morgan, A. Mujinga Mulumba, P. Mukadi Kakoni, D. Mukadi-Bamuleka, J.-J. Muyembe, N. T. Bathé, P. Ndumbi Ngamala, R. Ngom, G. Ngoy, P. Nouvellet, J. Nsio, K. B. Ousman, E. Peron, J. A. Polonsky, M. J. Ryan, A. Touré, R. Towner, G. Tshapenda, R. Van De Weerd, M. Van Kerkhove, A. Wendland, N. K. M. Yao, Z. Yoti, E. Yuma, G. Kalambayi Kabamba, J. deD. Lukwesa Mwati, G. Mbuy, L. Lubula, A. Mutombo, O. Mavila, Y. Lay, E. Kitenge, *Lancet* **2018**, *392*, 213.
- [11] Z. Yang, H. J. Duckers, N. J. Sullivan, A. Sanchez, E. G. Nabel, G. J. Nabel, *Nat. Med.* **2000**, *6*, 886.
- [12] World Health Organization (WHO), Ebola health update – DRC, **2019**, <https://www.who.int/emergencies/diseases/ebola/drc-2019>.
- [13] H. Rohde, J. Qin, Y. Cui, D. Li, N. J. Loman, M. Hentschke, W. Chen, F. Pu, Y. Peng, J. Li, F. Xi, S. Li, Y. Li, Z. Zhang, X. Yang, M. Zhao, P. Wang, Y. Guan, Z. Cen, X. Zhao, M. Christner, R. Kobbe, S. Loos, J. Oh, L. Yang, A. Danchin, G. F. Gao, Y. Song, Y. Li, H. Yang, J. Wang, J. Xu, M. J. Pallen, J. Wang, M. Aepfelbacher, R. Yang, *N. Engl. J. Med.* **2011**, *365*, 718.
- [14] A. Mellmann, D. Harmsen, C. A. Cummings, E. B. Zentz, S. R. Leopold, A. Rico, K. Prior, R. Szczepanowski, Y. Ji, W. Zhang, S. F. McLaughlin, J. K. Henkhaus, B. Leopold, M. Bielaszewska, R. Prager, P. M. Brzoska, R. L. Moore, S. Guenther, J. M. Rothberg, H. Karch, *PLoS One* **2011**, *6*, e22751.
- [15] M. Bielaszewska, A. Mellmann, W. Zhang, R. Köck, A. Fruth, A. Bauwens, G. Peters, H. Karch, *Lancet Infect. Dis.* **2011**, *11*, 671.
- [16] L. Kunsmann, C. Rüter, A. Bauwens, L. Greune, M. Glüder, B. Kemper, A. Fruth, S. N. Wai, X. He, R. Lloubes, M. A. Schmidt, U. Dobrindt, A. Mellmann, H. Karch, M. Bielaszewska, *Sci. Rep.* **2015**, *5*, 13252.
- [17] R. R. Muder, V. L. Yu, A. H. Woo, *Arch. Intern. Med.* **1986**, *146*, 1607.
- [18] D. M. Bitar, M. Molmeret, Y. Abu Kwaik, *Int. J. Med. Microbiol.* **2004**, *293*, 519.
- [19] S. Bartfeld, C. Engels, B. Bauer, P. Aurass, A. Flieger, H. Brüggemann, T. F. Meyer, *Cell. Microbiol.* **2009**, *11*, 1638.
- [20] S. T. Bagley, *Infect. Control Hosp. Epidemiol.* **1985**, *6*, 52.
- [21] C. Struve, K. A. Krogfelt, *FEMS Microbiol. Lett.* **2003**, *218*, 149.
- [22] S. Brisse, V. Passet, P. A. D. Grimont, *Int. J. Syst. Evol. Microbiol.* **2014**, *64*, 3146.
- [23] M. J. Delincé, J.-B. Bureau, A. Teresa López-Jiménez, P. Cosson, T. Soldati, J. D. McKinney, *Lab Chip* **2016**, *16*, 3276.
- [24] F. D. Lowy, *N. Engl. J. Med.* **1998**, *339*, 520.
- [25] Y. L. Loir, M. Gautier, in *Encyclopedia of Molecular Mechanisms of Disease* (Ed.: F. Lang), Springer, Berlin, Heidelberg, **2009**, pp. 1974–1975.
- [26] T. J. Foster, M. Höök, *Trends Microbiol.* **1998**, *6*, 484.
- [27] D. Baldoni, H. Hermann, R. Frei, A. Trampuz, A. Steinhuber, *J. Clin. Microbiol.* **2009**, *47*, 774.
- [28] World Health Organization (WHO), Coronavirus Disease (COVID-19) – events as they happen, <https://www.who.int/emergencies/diseases/ebola/drc-2019>.
- [29] B. Náfrádi, G. Náfrádi, C. Martin-Hamka, L. Forró, E. Horváth, *Langmuir* **2017**, *33*, 9043.
- [30] T. Matsunaga, R. Tomoda, T. Nakajima, H. Wake, *FEMS Microbiol. Lett.* **1985**, *29*, 211.
- [31] R. J. Watts, S. Kong, M. P. Orr, G. C. Miller, B. E. Henry, *Water Res.* **1995**, *29*, 95.
- [32] J. A. Herrera Melián, J. M. Doña Rodríguez, A. Viera Suárez, E. Tello Rendón, C. Valdés do Campo, J. Arana, J. Pérez Peña, *Chemosphere* **2000**, *41*, 323.

- [33] J. Araña, J. A. Herrera Melián, J. M. Doña Rodríguez, O. González Díaz, A. Viera, J. Pérez Peña, P. M. Marrero Sosa, V. Espino Jiménez, *Catal. Today* **2002**, 76, 279.
- [34] P. S. M. Dunlop, J. A. Byrne, N. Manga, B. R. Eggins, *J. Photochem. Photobiol. A: Chem.* **2002**, 148, 355.
- [35] J. A. Ibáñez, M. I. Litter, R. A. Pizarro, *J. Photochem. Photobiol. A: Chem.* **2003**, 157, 81.
- [36] G. Gogniat, M. Thyssen, M. Denis, C. Pulgarin, S. Dukan, *FEMS Microbiol. Lett.* **2006**, 258, 18.
- [37] N. Tétreault, E. Horváth, T. Moehl, J. Brillet, R. Smajda, S. Bungener, N. Cai, P. Wang, S. M. Zakeeruddin, L. Forró, A. Magrez, M. Grätzel, *ACS Nano* **2010**, 4, 7644.
- [38] M. Rosales, T. Zoltan, C. Yadarola, E. Mosquera, F. Gracia, A. García, *J. Mol. Liq.* **2019**, 281, 59.
- [39] K. Nakata, A. Fujishima, *J. Photochem. Photobiol., C* **2012**, 13, 169.
- [40] K. Mantulnikovs, P. Szirmai, M. Kollár, J. Stevens, P. Andričević, A. Glushkova, L. Rossi, P. Bugnon, E. Horváth, A. Sienkiewicz, L. Forró, B. Náfrádi, *J. Phys.: Photon.* **2020**, 2, 014007.
- [41] J. Nie, Z. Ren, Y. Bai, J. Shao, T. Jiang, L. Xu, X. Chen, Z. L. Wang, *Adv. Mater. Technol.* **2019**, 4, 1800300.
- [42] E. Horváth, L. Forró, A. Magrez, Titanium oxide aerogel composites *US Patent No. US2016030908 (A1)*, **2016**.
- [43] E. Horváth, Á. Kukovecz, Z. Kónya, I. Kiricsi, *Chem. Mater.* **2007**, 19, 927.
- [44] E. Horváth, P. R. Ribič, F. Hashemi, L. Forró, A. Magrez, *J. Mater. Chem.* **2012**, 22, 8778.
- [45] P. Szirmai, B. Náfrádi, A. Arakcheeva, E. Szilágyi, R. Gaál, N. M. Nemes, X. Berdat, M. Spina, L. Bernard, J. Jačimović, A. Magrez, L. Forró, E. Horváth, *Catal. Today* **2017**, 284, 52.
- [46] P. Szirmai, J. Stevens, E. Horváth, L. Čirić, M. Kollár, L. Forró, B. Náfrádi, *Catal. Today* **2017**, 284, 146.
- [47] T. Szabó, V. Tóth, E. Horváth, L. Forró, I. Szilágyi, *Langmuir* **2015**, 31, 42.
- [48] L. Rossi, X. Berdat, M. Spina, S. Brown, L. Bernard, S. Katrych, L. Forró, E. Horváth, *Ceram. Int.* **2020**, 46, 16321.
- [49] L. Rossi, R. Foschia, A. Glushkova, L. Forró, E. Horváth, *Ceram. Int.* **2020**, 46, 17729.
- [50] J. Jačimović, C. Vaju, A. Magrez, H. Berger, L. Forró, R. Gaál, V. Cerovski, R. Žikić, *Europhys. Lett.* **2012**, 99, 57005.
- [51] Y. Nosaka, A. Y. Nosaka, *Chem. Rev.* **2017**, 117, 11302.
- [52] M. Chen, J. Ma, B. Zhang, F. Wang, Y. Li, C. Zhang, H. He, *Appl. Catal., B* **2018**, 223, 209.
- [53] J. C. Ireland, P. Klostermann, E. W. Rice, R. M. Clark, *Appl. Environ. Microbiol.* **1993**, 59, 1668.
- [54] M. Cho, H. Chung, W. Choi, J. Yoon, *Appl. Environ. Microbiol.* **2005**, 71, 270.
- [55] V. Marchand, N. Charlier, J. Verrax, P. Buc-Calderon, P. Levêque, B. Gallez, *PLoS One* **2017**, 12, e0172998.
- [56] H. Lu, J. Zhen, T. Wu, A. Peng, T. Ye, T. Wang, X. Yu, N. D. Vaziri, C. Mohan, X. J. Zhou, *Am. J. Physiol.-Renal Physiol.* **2010**, 299, F445.
- [57] C. S. Wilcox, *Pharmacol. Ther.* **2010**, 126, 119.
- [58] D. L. Marshall, M. L. Christian, G. Gryn'ova, M. L. Coote, P. J. Barker, S. J. Blanksby, *Org. Biomol. Chem.* **2011**, 9, 4936.
- [59] N. H. L. Leung, D. K. W. Chu, E. Y. C. Shiu, K.-H. Chan, J. J. McDevitt, B. J. P. Hau, H.-L. Yen, Y. Li, D. K. M. Ip, J. S. M. Peiris, W.-H. Seto, G. M. Leung, D. K. Milton, B. J. Cowling, *Nat. Med.* **2020**, 26, 676.
- [60] The EPFL's invention awarded second place by the UAE's 28 Water Aid Foundation **2017**, <https://www.suqia.ae>.